

This article was downloaded by:

On: 25 January 2011

Access details: *Access Details: Free Access*

Publisher *Taylor & Francis*

Informa Ltd Registered in England and Wales Registered Number: 1072954 Registered office: Mortimer House, 37-41 Mortimer Street, London W1T 3JH, UK



## Liquid Crystals

Publication details, including instructions for authors and subscription information:

<http://www.informaworld.com/smpp/title~content=t713926090>

### Nematic structures in cylindrical cavities

A. M. Smondyrev

Online publication date: 06 August 2010

**To cite this Article** Smondyrev, A. M.(1999) 'Nematic structures in cylindrical cavities', *Liquid Crystals*, 26: 2, 235 – 240

**To link to this Article:** DOI: 10.1080/026782999205371

**URL:** <http://dx.doi.org/10.1080/026782999205371>

PLEASE SCROLL DOWN FOR ARTICLE

Full terms and conditions of use: <http://www.informaworld.com/terms-and-conditions-of-access.pdf>

This article may be used for research, teaching and private study purposes. Any substantial or systematic reproduction, re-distribution, re-selling, loan or sub-licensing, systematic supply or distribution in any form to anyone is expressly forbidden.

The publisher does not give any warranty express or implied or make any representation that the contents will be complete or accurate or up to date. The accuracy of any instructions, formulae and drug doses should be independently verified with primary sources. The publisher shall not be liable for any loss, actions, claims, proceedings, demand or costs or damages whatsoever or howsoever caused arising directly or indirectly in connection with or arising out of the use of this material.

# Nematic structures in cylindrical cavities

A. M. SMONDYREV

Department of Chemistry, University of North Carolina at Chapel Hill,  
Chapel Hill, NC 27599, USA

and ROBERT A. PELCOVITS\*

Department of Physics, Brown University, Providence, RI 02912, USA

(Received 31 August 1998; accepted 17 September 1998)

We present the results of Monte Carlo simulations of a nematic liquid crystal confined to a cylinder with homeotropic surface anchoring. The nematic is modelled using the Lebwohl–Lasher model. For low values of the cylinder radius or anchoring strength, a stable planar polar configuration with two line defects is readily formed, consistent with the predictions of elastic theory. At larger values of the radius or anchoring strength we observe a metastable escaped radial configuration. However, this structure eventually collapses to a planar configuration, contrary to the predictions of elastic theory.

## 1. Introduction

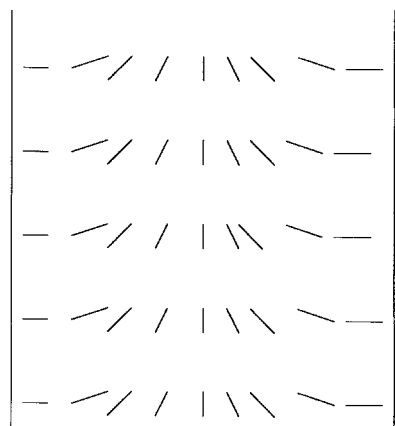
Liquid crystals confined to cylindrical cavities with homeotropic radial boundary conditions can exhibit a variety of nontrivial structures depending on the competition between bulk elastic and surface energies. By minimizing the Frank elastic free energy Cladis and Kleman [1] and Meyer [2] showed that for a cylinder with a sufficiently large radius an escaped radial (ER) configuration will form. This configuration can be thought of as a planar radial (PR) structure (i.e. a disclination line) which has ‘escaped’ along the axis of the cylinder (see figure 1). Later studies [3] showed the possibility of additional structures including planar polar (PP) and planar polar with two line defects (PPLD). In these latter configurations the director lies in a plane perpendicular to the axis of the cylinder with a strong component along a single in-plane direction (see figure 2). In the PP structure the local director is uniform near the axis of the cylinder and radial at the boundary. In the PPLD structure there are two half-integer disclination lines parallel to the cylinder axis.

Kralj and Zumer [4] carried out a very complete numerical stability analysis of the various nematic structures in a cylindrical geometry by minimizing the Frank elastic energy (including the saddle–splay elastic constant  $K_{24}$ ). For most values of the elastic constants they found a phase diagram with ER and PP structures, with the ER structure stable for large radii and/or strong

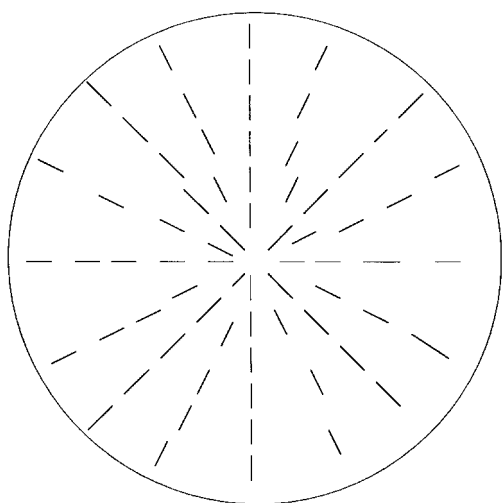
anchoring. In particular if the twist and splay elastic constants are equal and  $K_{24} = 0$ , then the ER structure should form when  $RW/K$  exceeds about 27, where  $R$ ,  $W$  and  $K$  are the cylinder radius (measured in units of intermolecular spacing), anchoring strength, and Frank elastic constant, respectively. However, a PR structure appears if the twist constant is very large compared with splay. They also found that the PPLD structure can be stabilized if  $K_{24}$  is nearly zero,  $R$  is approximately 100, and the half-integer defect lines are separated by a distance equal to the diameter of the cylinder. An analytic study of these director structures has recently been carried out [5] with similar results.

Monte Carlo (MC) simulations of a cylindrically confined nematic with radial homeotropic boundary conditions were first performed by Chiccoli *et al.* [6]. They used a Lebwohl–Lasher lattice model [7], and studied cylinders of radii 6 and 11 lattice spacings and heights  $h = 40, 52, 62, 82$  lattice spacings, with periodic boundary conditions along the cylindrical axis dimension. Various values of the ratio of the surface anchoring strength  $\varepsilon_s$  to the bulk nearest-neighbour coupling  $\varepsilon_b$  were considered, the largest being unity. In all cases, a planar structure was observed; however, these authors did not determine whether this structure is PP or PPLD. Surprisingly an ER structure was never produced in these simulations. If we assume (possibly incorrectly) that the ratio  $\varepsilon_s/\varepsilon_b$  equals the corresponding Frank elastic energy ratio  $W/K$ , then according to the analysis of ref. [4], the ER structure should form for  $R$  greater than approximately 27. According to Chiccoli *et al.*,

\*Author for correspondence.



(a)

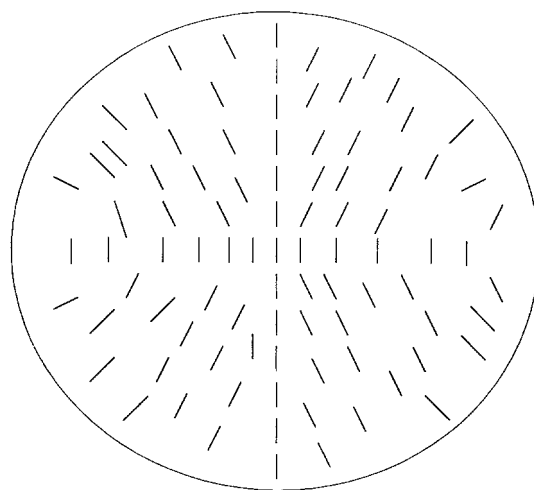


(b)

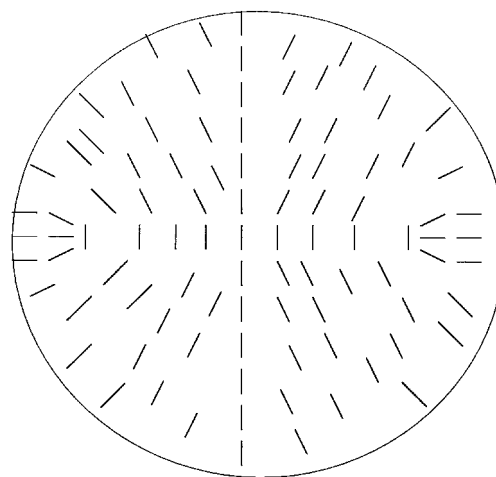
Figure 1. Schematic director pattern in the (a) escaped radial (ER), and (b) planar radial (PR) configurations. The cylinder axis is vertical in (a) and perpendicular to the page in (b).

each Lebwohl–Lasher spin typically corresponds to about 10 molecules; so for a cylinder of radius 4 lattice spacings, an ER configuration should have been seen in these simulations.

In this paper we consider a similar Lebwohl–Lasher model of a nematic confined to a cylinder. In an attempt to produce the stable ER configuration predicted by elastic theory at large values of the radius we have simulated cylinders of radii up to 160 lattice spacings but with heights as low as 16 spacings [8]. At small radii we find a stable planar structure which we are able to characterize as a PPLD configuration; this result is consistent with elastic theory. For larger values of the radius (well beyond the threshold value predicted by elastic theory [4]) we find a *metastable* escaped radial



(a)



(b)

Figure 2. Schematic director pattern in the (a) planar polar (PP), and (b) planar polar with line defects (PPLD) configurations. The cylinder axis is perpendicular to the page.

configuration. However, this escaped configuration ultimately collapses to a planar state, after approximately 150 000 MC steps.

In the next section we present the details of our model; this is followed by a section describing the simulations. We discuss the apparent lack of agreement of our results with elastic theory in the final section.

## 2. Model

We use a cylinder geometry variant of the Lebwohl–Lasher model, identical to the one employed by Chiccoli *et al.* [6]. The Lebwohl–Lasher model represents each mesogenic molecule or small group of molecules by a three-dimensional spin vector. These spins are free to

rotate about their centres which are fixed on the sites of a simple cubic lattice. To simulate a system of spins in a cylinder we introduce two types of spins depending on their distance from the centre of the cylinder. Spins whose distance  $r$  from the centre of the cylinder is less than  $R$ , the radius of the cylinder, are free to rotate and interact with their nearest-neighbours through the usual Lebwohl–Lasher pair potential:

$$U_{ij} = -\varepsilon_b P_2(\cos \theta_{ij}) \quad (1)$$

where  $\theta_{ij}$  is the angle between two spins  $i$  and  $j$ ,  $P_2$  is a second rank Legendre polynomial and  $\varepsilon_b$  is a positive constant for nearest neighbour sites and zero otherwise. Spins located at distances  $R < r < R_c$  have a fixed direction and do not move. These spins represent the boundary and their direction was chosen to point towards the centre of the cylinder to simulate homeotropic boundary conditions. The outer radius  $R_c$  was chosen to ensure that all spins inside the cylinder (i.e. with  $r < R$ ) have a total of six nearest-neighbours, whether from the interior or the boundary. The interaction of the boundary spins with the spins inside the cylinder is described by the potential:

$$U_{ik} = -\varepsilon_s P_2(\cos \theta_{ik}) \quad (2)$$

where spin  $i$  is located inside the cylinder and spin  $k$  is the nearest neighbour spin which belongs to the boundary layer. The coupling  $\varepsilon_s$  is the surface anchoring strength. The total potential energy is given by the sum of the two energies above, summed over all pairs of spins. Note that in the Lebwohl–Lasher model, because the energy is invariant under a uniform rotation of all the spins, the bend, splay and twist elastic constants are equal, and the saddle–splay elastic constant  $K_{24}$  is identically zero.

### 3. Simulation

To perform MC simulations of the above model, we divided all of the spins into two sublattices, such that all the nearest neighbours of a spin located on sublattice A belong to sublattice B. Each MC step in our simulation corresponds to one attempted move per spin. First we try to move spins on sublattice A and then spins on sublattice B. This sequence helps us to avoid possible collective motions of neighbouring spins. We also performed the simulations with random sequencing of sites with no change in our final results. The amplitudes of trial moves were adjusted to give a rejection ratio around 0.5. We studied systems placed in cylinders of radii ranging from  $R = 20$  to  $R = 160$ , with heights ranging from 16 for the largest radii to 20 for the smallest radii (all distances are measured in lattice spacings). Our initial configuration was typically a system of randomly oriented spins at temperature  $T^* = 1.3$  ( $T^* = kT/\varepsilon_b$ ),

corresponding to the isotropic phase; however, our final configurations were essentially the same even when beginning with an escaped configuration. The temperature was then lowered in steps of 0.1 to  $T^* = 0.9$ . At each temperature the system was allowed to equilibrate for 50 000 MC steps, though for the larger radii we ran the simulations for an additional 120 000 steps. In addition to the usual nematic order parameter  $P_2$  calculated from the largest eigenvalue of the ordering matrix, we calculated two additional order parameters, radial and escaped. We define a radial order parameter [6] by:

$$P_2^{\text{rad}} = (1/N) \sum P_2(\hat{\mathbf{u}}_i \cdot \hat{\mathbf{n}}_i) \quad (3)$$

where  $\hat{\mathbf{u}}_i$  is an orientation vector of spin  $i$ ,  $\hat{\mathbf{n}}_i$  is a local unit vector pointing towards the centre of the cylinder, and  $N$  is the number of spins in the cylinder. The sum is over all spins in the cylinder. In a perfect PR configuration  $P_2^{\text{rad}}$  would be unity. We also introduce an escaped order parameter, which measures the degree of spin tilt away from the plane perpendicular to the cylinder axis. It is given by:

$$P_2^{\text{esc}} = (1/N) \sum P_2(\hat{\mathbf{u}}_i \cdot \hat{\mathbf{z}}) \quad (4)$$

where the cylinder axis is along the  $z$  direction. The escaped order parameter is calculated as a function of the distance from the centre of the cylinder, and the sum is over spins in a thin annulus with the same height as the cylinder.

The values of  $P_2$  and  $P_2^{\text{rad}}$  for different temperatures and cylinder radii are shown in the table. In figure 3 we plot results for the escaped order parameter  $P_2^{\text{esc}}$  for systems of radii 80 and 160 as a function of the distance from the centre of the cylinder at a temperature of  $T^* = 0.9$  (note that the data presented for the larger radius cylinder is for the first 50 000 MC steps). For the system of radius  $R = 80$  (where we used  $\varepsilon_s = 0.5$ ) the escaped order parameter remains negative for all values of  $r$ , and is approximately equal to  $-1/3$ . According to our definition, equation (4), this implies that the spins on average make an angle of approximately  $70^\circ$  with the  $z$  axis, i.e. it is a nearly planar structure. We have simulated smaller systems at lower temperatures and found values of  $P_2^{\text{esc}}$  progressively approaching  $-0.5$ , which is the value for a perfectly planar structure. The system of radius  $R = 160$  (where we used  $\varepsilon_s = 1.0$ ) exhibits completely different features, over a range of 50 000–100 000 MC steps. Spins which lie closer to the cylinder axis are more significantly tilted towards the cylinder axis, while the spins closer to the outer boundary of the cylinder are oriented perpendicular to the cylinder axis. This behaviour is characteristic of an escaped radial configuration. However, after approximately 100 000 MC steps this structure began to collapse to a planar configuration similar to the one observed at a radius of 80.

Table. The nematic order parameter  $P_2$  and the radial order parameter  $P_2^{\text{rad}}$ , equation (3), as functions of temperature for cylinders of radii 80 and 160 lattice spacings. Note that for the theoretical ER configuration, a brief calculation shows that the nematic order parameter has the value 0.159.

$T^*$	$R = 80$		$R = 160$	
	$P_2$	$P_2^{\text{rad}}$	$P_2$	$P_2^{\text{rad}}$
1.3	$0.008 \pm 0.002$	$0.265 \pm 0.003$	$0.006 \pm 0.001$	$0.260 \pm 0.001$
1.2	$0.011 \pm 0.002$	$0.270 \pm 0.003$	$0.010 \pm 0.001$	$0.266 \pm 0.002$
1.1	$0.115 \pm 0.043$	$0.486 \pm 0.049$	$0.055 \pm 0.020$	$0.408 \pm 0.039$
1.0	$0.284 \pm 0.014$	$0.611 \pm 0.009$	$0.074 \pm 0.007$	$0.543 \pm 0.015$
0.9	$0.364 \pm 0.008$	$0.628 \pm 0.004$	$0.105 \pm 0.007$	$0.615 \pm 0.008$

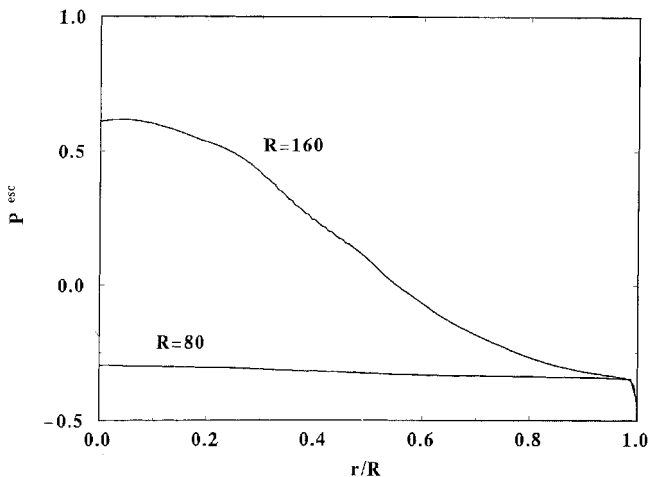


Figure 3. Plot of the escaped order parameter  $P_2^{\text{esc}}$ , equation (4), as a function of the scaled distance from the cylinder axis for radii 80 and 160. The data for the large radius is from the first 50 000 MC steps; ultimately this structure collapsed to a planar configuration.

This latter state has essentially the same energy as the escaped state; unfortunately calculating the free energy difference would take a prohibitively large amount of computer time.

We also simulated a system of radius  $R = 160$ , but with lower anchoring strength  $\varepsilon_s = 0.25$ . In this simulation we readily obtained a planar structure which was very similar to the one obtained when the cylinder radius was  $R = 80$ , and  $\varepsilon_s = 0.5$ . For both of these systems the ratio  $R\varepsilon_s/\varepsilon_b$  is 40. According to elastic theory [4], the relative stability of the ER and planar configurations depends on the value of  $RW/K$ , i.e. the ‘renormalized’ value of our ratio,  $R\varepsilon_s/\varepsilon_b$ . So our result that two systems with different radii and anchoring strengths, but with the same value of  $R\varepsilon_s/\varepsilon_b$ , have similar behaviour is consistent with elastic theory. Furthermore, our result is consistent with the prediction of elastic theory, that systems with relatively small radii or weak anchoring strength yield planar configurations.

To probe the observed planar structure we calculated an ‘in-plane’ order parameter defined by:

$$P_2^{xy}(r) = \langle P_2(\hat{\mathbf{u}}; \hat{\mathbf{h}}) \rangle \quad (5)$$

where  $\langle \rangle$  denotes an average over the spins in a narrow slice perpendicular to the cylinder axis and parallel to a vector  $\hat{\mathbf{h}}$  lying in a plane perpendicular to the cylinder axis. In figure 4 we plot results for the ‘in-plane’ order parameter for a system of radius  $R = 20$  as a function of the distance from the centre of the cylinder for two mutually perpendicular directions of  $\hat{\mathbf{h}}$ . These plots are consistent with a PPLD structure, see figure 2(b). For  $\hat{\mathbf{h}}$  parallel to the average director we see that  $P_2^{xy}(r)$  fluctuates around a constant value and does not depend on the distance from the cylinder axis. For  $\hat{\mathbf{h}}$  perpendicular to the nematic director the ‘in-plane’ order parameter is negative and close to  $-0.5$  near the centre of the cylinder (indicating that most spins are perpendicular to  $\hat{\mathbf{h}}$ ), while

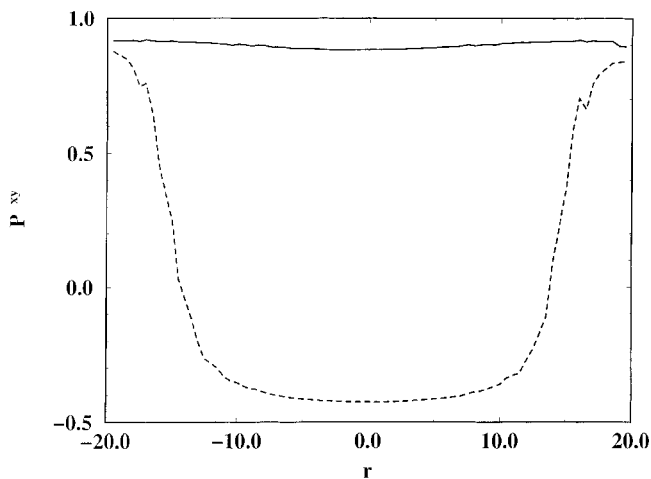


Figure 4. Plot of the in-plane order parameter  $P_2^{xy}$ , equation (5), as a function of the scaled distance from the cylinder axis for radius 20. The solid line corresponds to the vector  $\hat{\mathbf{h}}$  [see equation (5)] parallel to the average director, while the dashed line corresponds to  $\hat{\mathbf{h}}$  perpendicular to the director. These plots are consistent with a PPLD structure, see figure 2(b).

near the surface of the cylinder the spins are mostly parallel to  $\hat{\mathbf{h}}$  due to surface anchoring. The transition between the two regions is rather sharp and gives the approximate sizes of the two opposite line defects.

Another method for identifying director structures inside cylindrical cavities is NMR [3]. We calculated NMR spectra from our simulation data for two orientations of the cylinder axis in a magnetic field (parallel and perpendicular) using a procedure described in [9]. A single spin will yield a spectrum of two lines at frequencies  $\nu_0$  given by:

$$\nu_0(r) = \pm \frac{S\nu_Q}{2} (3 \cos^2 \theta(r) - 1) \quad (6)$$

where  $\theta(r)$  is the angle between the direction of the spin at site  $r$  and the magnetic field,  $\nu_Q$  is the quadrupole splitting constant and  $S = 1/2 \langle 3 \cos^2 \alpha - 1 \rangle$  is the degree of orientational order of the quadrupole axis with respect to the molecular axis. The total spectrum is calculated as an average over several configurations:

$$S(\nu) = \frac{1}{N} \sum S(\nu, \nu_0(r)) \quad (7)$$

where the summation is done over all spins. We assume that each line has a Lorentzian shape:

$$S(\nu, \nu_0(r)) = \frac{T_2^{-1}}{(\nu - \nu_0(r))^2 + (T_2^{-1})^2} + \frac{T_2^{-1}}{(\nu + \nu_0(r))^2 + (T_2^{-1})^2} \quad (8)$$

where  $T_2^{-1}$  is the intrinsic line width. We adopted for  $T_2^{-1}$ ,  $\nu_Q$  and  $\alpha$  the values used by Berggren *et al.* [9];

our results for  $S(\nu)$  are in arbitrary units. Spectral shapes for systems of radii 20 (anchoring strength  $\varepsilon_s = 0.5$ ) and 160 (anchoring strength  $\varepsilon_s = 1.0$ , and data taken from the metastable ER configuration) are shown in figure 5. In the case of the planar structure ( $R = 20$ ) with the cylinder axis oriented parallel to the magnetic field, we observe a single sharp peak because all spins are almost planar so that the angles  $\theta(r)$  are close to  $90^\circ$ . With the magnetic field oriented parallel to the symmetry axis of the planar configuration and perpendicular to the cylinder axis the separation between peaks increases. In this case the two line defects are symmetrical mirror images and almost all spins lie parallel to the magnetic field. The smaller peaks are due to the two line defects. It should be noted that the main peak is relatively wide and its intensity varies if the orientation of the magnetic field is changed. For the metastable escaped structure ( $R = 160$ ) the splitting of the main peaks is the same for both orientations of the magnetic field. When the magnetic field is rotated in a plane perpendicular to the cylinder axis the amplitude of the main peak does not change. This indicates that the structure has radial symmetry. Another feature which is typical of an escaped structure is that the probability of  $\nu$  having values between 0 and 1.0 is non-zero whereas  $\nu$  is zero for planar structure. These features were observed both in experiments and simulates spectral patterns in the strong anchoring limit [11].

#### 4. Discussion

We now discuss the status of the agreement, or lack thereof, or our results with those of elastic theory.

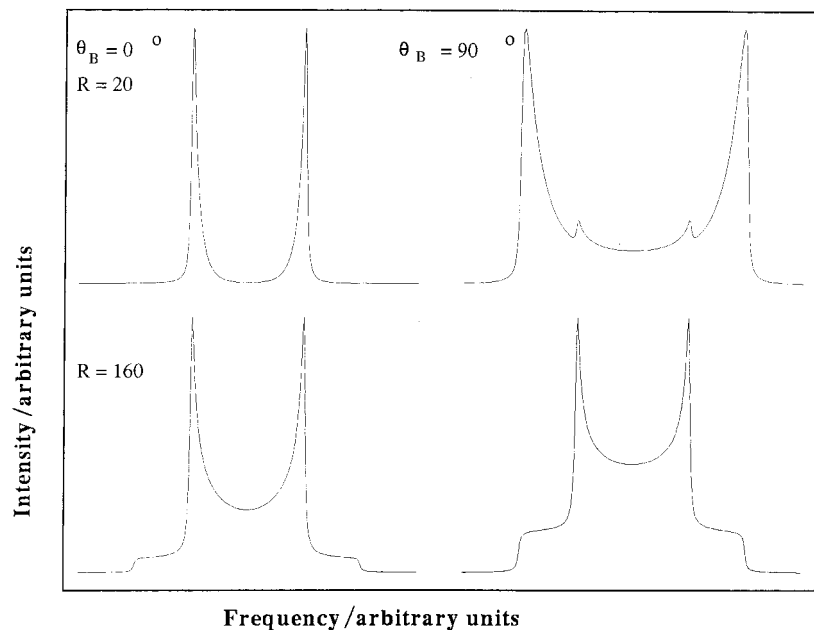


Figure 5. NMR spectral shapes, equation (7), for cylinders of radii 20 and 160, and magnetic field oriented perpendicular to the cylinder axis ( $\theta_B = 0^\circ$ ) and parallel to the cylinder axis ( $\theta_B = 90^\circ$ ). The data is normalized so that the peaks in the four plots have the same height. Note that the data for the system of radius 160 is from the first 50 000 MC steps, before the ER structure collapsed to a planar configuration.

According to elastic theory [4], an ER structure should form for values of  $RW/K > 27$  (for the parameters of the Lebwohl–Lasher model), with a planar structure forming for smaller values. We have indeed found a planar structure (PPLD specifically) at relatively low values of  $R\epsilon_s/\epsilon_b$ , irrespective of the choice of  $R$ ; in this way our results are consistent with the predictions of elastic theory. However, for  $R\epsilon_s/\epsilon_b$  even as large as 160, we have been unable to produce a *stable* ER configuration, though we did produce a metastable ER state. While most of our runs were performed starting with a random initial configuration we did carry out runs starting with an ER configuration and again found a collapse to a planar state. Possibly the discrepancy with the predictions of elastic theory arises from equating  $RW/K$  with our ‘bare’ ratio,  $R\epsilon_s/\epsilon_b$ . The temperature dependence of the Frank elastic constant  $K$  has been measured in the Lebwohl–Lasher model by Cleaver and Allen [11], however, there have been no corresponding measurements of the surface anchoring parameter  $W$ . Thus, it is not clear if the ratio  $RW/K$  is temperature independent and equal in value to  $R\epsilon_s/\epsilon_b$ , the parameter set in our simulations. If  $RW/K$  were temperature independent then our results suggest that the critical value of  $RW/K$  for the formation of an ER configuration is significantly higher than 27, in fact in excess of 160. We would attribute this disagreement with elastic theory to the presence of thermal fluctuations in our simulations (note, however, that we were unable to produce a stable ER configuration even at lower temperatures). Another possibility is that  $RW/K$  has significant temperature dependence, and while we set our parameter  $R\epsilon_s/\epsilon_b = 160$ , this corresponds to a much lower value of  $RW/K$ . Of

course, it is also possible that even with a significant temperature dependence of  $RW/K$ , thermal fluctuations still modify the threshold value of this parameter. Clearly more exploration of this problem is warranted.

We are grateful to Prof. G. P. Crawford for helpful discussions, and to Dr G. Loriot for computational assistance. This work was supported by the National Science Foundation under grant no. DMR-9528092. Computational work was performed at the Theoretical Physics Computing Facility at Brown University.

### References

- [1] CLADIS, P. E., and KLEMAN, M., 1972, *J. Phys. (Paris)*, **33**, 591.
- [2] MEYER, R. B., 1973, *Phil. Mag.*, **27**, 405.
- [3] ALLENDER, D. W., CRAWFORD, G. P., and DOANE, J. W., 1991, *Phys. Rev. Lett.*, **67**, 1442; CRAWFORD, G. P., ALLENDER, D. W., and DOANE, J. W., 1992, *Phys. Rev. A*, **45**, 8693; KRALJ, S., and ŽUMER, 1992, *Phys. Rev. A*, **45**, 2461; KRALJ, S., and ŽUMER, S., 1993, *Liq. Cryst.*, **15**, 521.
- [4] KRALJ, S., and ŽUMER, S., 1995, *Phys. Rev. E*, **51**, 366.
- [5] BURYLOV, S. V., 1997, *Sov. Phys. JETP*, **85**, 873.
- [6] CHICCOLI, C., PASINI, P., SEMEIRA, F., BERGGREN, E., and ZANNONI, C., 1996, *Mol. Cryst. liq. Cryst.*, **290**, 237.
- [7] LEBWOHL, P. A., and LASHER, G., 1972, *Phys. Rev. A*, **50**, 4780.
- [8] Note that even for  $R = 160$  we are still well below the length scales at which spin waves destroy the nematic order in a system of thickness 16. See, e.g., Cleaver, D. J., and Allen, M. P., 1993, *Mol. Phys.*, **80**, 253.
- [9] BERGGREN, E., ZANNONI, C., CHICCOLI, C., PASINI, P., and SEMERA, F., 1994, *Phys. Rev. E*, **49**, 614.
- [10] CRAWFORD, G. P., ALLENDER, D. W., DOANE, J. W., VILFAN, M., and VILFAN, I., 1991, *Phys. Rev. A*, **44**, 2570.
- [11] CLEAVER, D. J., and ALLEN, M. P., 1991, *Phys. Rev. A*, **43**, 1918.